

¹ Physical Chemistry II,

² Macromolecular Chemistry I,

University of Bayreuth, D-W-8580 Bayreuth, Germany,

³ Laser-Laboratorium Göttingen, D-W-3400 Göttingen, Germany

Triazene polymers designed for excimer laser ablation

Th. Lippert¹, A. Wokaun^{1*}, J. Stebani², O. Nuyken², J. Ihlemann³

(Received 8 July 1992)

SUMMARY:

The excimer laser-induced ablation of triazene polymers at a wavelength of 308 nm has been investigated as a function of laser fluence deposited on the surface in one or several pulses. PMMA, which as a homopolymer can not be ablated at 308 nm, has been sensitized for ablation at this wavelength by synthesizing a copolymer in which 0.3 mol-% of the side chains contain the triazene functional groups. The high ablated depths per pulse achieved in this manner are similar to the ones observed upon physical doping of PMMA with monomeric triazene compounds. In an alternative approach, the triazene functional group is introduced once (polymer TP 1) or twice (TP 2) into each repeating unit of the polymer backbone by a polycondensation reaction. Irradiation of TP 1 gives rise to ill-defined ablation profiles with sloping wall. In contrast, clean circular ablation profiles are obtained with polymer TP 2, which are characterized by circular contours, steep edges, and flat bottoms of the ablated craters. The origins of these differences are investigated. A comparative study of excimer laser ablation of TP 2 at 248 and 308 nm shows that the latter wavelength is more effective; the plateau value of the ablated depth per pulse corresponds to $\approx 1 \mu\text{m}$ at 248 nm and $\approx 3 \mu\text{m}$ at 308 nm. This dependence is attributed to the photolysis behaviour of the triazene compounds: nitrogen released upon photolytic bond cleavage acts as a driving gas which promotes the ablation. As a consequence, no 'incubation pulses' are required for triazene polymer ablation in the investigated fluence range.

ZUSAMMENFASSUNG:

Die Ablation von Triazenpolymeren durch Exzimerlaserpulse mit einer Wellenlänge von 308 nm wird als Funktion der auf der Oberfläche deponierten Energiedichte untersucht. Um PMMA, welches als Homopolymeres keine Absorption bei 308 nm aufweist, für die Ablation bei dieser Wellenlänge zu sensitivieren, wird ein PMMA-Copolymeres synthetisiert, in welchem ein Anteil von 0.3 mol-% der Seitengruppen die Triazengruppe enthält. An diesem Material beobachtet man Abtragtiefen von bis zu $\approx 30 \mu\text{m}$ pro Puls; das Ablationsverhalten des Copolymeren ist in dieser Hinsicht vergleichbar

* Correspondence author

mit demjenigen von PMMA, welches durch Lösen niedermolekularer Triazenverbindungen physikalisch dotiert wird.

Als Alternative zur Copolymerisation werden durch eine Polykondensationsreaktion Triazen-Hauptkettenpolymere mit einer bzw. zwei Triazengruppen pro Wiederholungseinheit synthetisiert (Polymere TP 1 bzw. TP 2). Während die Bestrahlung von TP 1 in unbefriedigenden Ablationsprofilen mit geneigten Kraterwänden resultiert, erhält man bei TP 2 gut definierte kreisförmige Profile mit scharfen Kanten, senkrechten Wänden und ebenen Böden der Ablationskrater. Ein Vergleich des Ablationsverhaltens von TP 2 bei 248 und 308 nm zeigt eine höhere Effizienz der Einstrahlung bei der größeren Wellenlänge: Der Grenzwert der Abtragtiefe pro Puls für hohe Laser-Energiedichten beträgt 1 μm bei 248 nm, im Vergleich zu 3 μm bei 308 nm. Diese Wellenlängenabhängigkeit wird auf den Mechanismus der Ablation im vorliegenden System zurückgeführt: Der bei der Photolyse der Triazene freigesetzte Stickstoff wirkt als 'Treibgas' für die Ablation. Als Konsequenz wird im Bereich der eingesetzten Laser-Energiedichten bereits beim ersten Puls Abtragung von Material beobachtet, d. h. es sind keine Inkubationspulse erforderlich.

Introduction

Since the first report in 1982^{1,2}, laser-induced ablation of polymers has been intensively studied. Nearly all polymers show an absorption in the UV region, and can therefore be ablated with an excimer laser. Wavelengths of 193 and 248 nm have been most commonly used for the structuring of polymer surfaces.

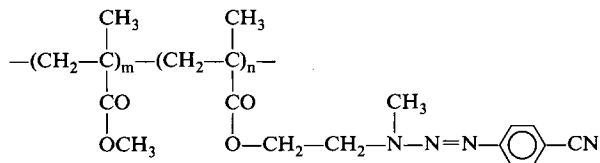
The 308 nm XeCl* excimer emission wavelength, which is attractive in view of stable, cost-effective high-power excimer laser operation, has rarely been used in laser ablation experiments. This is due to the fact that most polymers do not exhibit suitable absorption bands at 308 nm, and as a consequence can not be ablated at this wavelength in a controlled fashion to yield well defined surface structures with sharp edges and good resolution. An exception are polyimide materials which are successfully structured at 308 nm in industrial applications³.

One successful approach for sensitizing polymers such as PMMA, which do not exhibit an absorption at 308 nm, is the physical doping of these polymers with a small concentration of a suitable chromophore^{4,5}. This method is capable of producing well defined ablation structures. In the present study we are pursuing a complementary approach, i. e. the synthesis of polymers which contain the sensitizing chromophores. Three different types of polymers have been synthesized which are represented below. The copolymer I is synthesized by polymer-analogous reaction from an MMA/methacrylic acid chloride

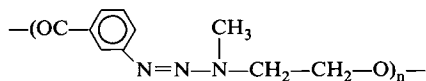
Triazene polymers designed for excimer laser ablation

copolymer; 0.3% of the side chains contain the triazene functionality. In contrast, the polymer TP 1 contains one triazene chromophore in the main chain for each repeating unit. Polymer TP 2, synthesized from the bis-diazonium ion of bis(4-aminophenyl)ether and N,N'-dimethylhexane-1,6-diamine, features two triazene groups per repeating unit.

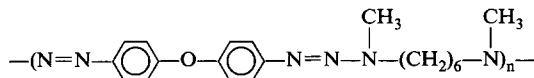
Scheme 1:



Copolymer I



Triazene polymer TP 1



Triazene polymer TP 2

Experimental

Instruments

Irradiations have been carried out using an excimer laser (Lambda Physik, model EMG 203 MSC) operated at a wavelength of 308 nm, with a pulse duration of ≈ 30 ns and a repetition rate of 2 Hz. Homogeneous irradiation of 375 μm -diameter areas on the sample was achieved by 9:1 imaging of a 3.2 mm-diameter circular diaphragm using a 100 mm focal length lens. The pulse energy incident on the sample was continuously adjusted by means of a variable attenuator (Laser-Laboratorium, Göttingen). The experimental setup has been described in detail elsewhere⁵.

¹H NMR spectra were recorded on a 250 MHz spectrometer (Bruker, model AC 250) with tetramethylsilane as internal standard. IR spectra were recorded on an FTIR instrument (Digilab, model FTS-40). Scanning electron micrographs were taken on a JEOL instrument (model JSM-840 A).

Synthesis of triazene monomers

1-(3-Carboxyphenyl)-3-(2-hydroxyethyl)-3-methyltriazene

1.37 g (0.01 mol) of 3-aminobenzoic acid is dissolved in 20 ml of a solution of 10% hydrochloric acid in distilled water and cooled to -5°C in a dry ice/acetone bath. A chilled solution of 0.69 g (0.01 mol) of sodium nitrite in 5 ml of distilled water is added under stirring, which is continued for 15 min. The resulting diazonium salt solution is added to a cooled solution of 6.0 g (0.08 mol) of 2-methylamino-ethanol in 100 ml of distilled water. The triazene product is precipitated from the deep-red solution by acidification to pH 4–5 with hydrochloric acid. The precipitate is filtered, washed with water, and dried in vacuo over diphosphorus pentoxide. The yield was 1.7 g (76%).

$^1\text{H NMR}$ (DMSO- d_6): $\delta = 3.2$ ppm (s; 3 H); 3.6–3.7 ppm (t; 2 H); 3.85–3.9 ppm (t; 2 H); 4.7–5.0 ppm (s; 1 H); 7.35–7.9 ppm (m; 4 H); 12.7–13.1 ppm (s; 1 H).

IR (KBr pellet): $\tilde{\nu} = 3200\text{--}2800$ cm^{-1} (—COOH; —OH); 1717 cm^{-1} (C=O).

UV/Vis (THF): $\lambda_{\text{max}} = 289$ nm; $\epsilon = 16300$ $\text{l mol}^{-1} \text{cm}^{-1}$.

| | | | | |
|---|-------|---------|--------|---------|
| $\text{C}_{10}\text{H}_{13}\text{N}_3\text{O}_3$ (223.23) | calc. | C 53.81 | H 5.87 | N 18.82 |
| | found | C 54.14 | H 5.90 | N 18.58 |

1-(4-Cyanophenyl)-3-(2-hydroxyethyl)-3-methyltriazene

1.18 g (0.01 mol) of 4-cyanoaniline is diazotized in a procedure analogous to the one described above. When the solution of 2-methylamino-ethanol is added to the diazonium salt solution, immediate precipitation of the triazene is observed. The precipitate is filtered, washed with water, and dried in vacuo over diphosphorus pentoxide. The yield was 1.3 g (63%).

$^1\text{H NMR}$ (DMSO- d_6): $\delta = 3.25$ ppm (s; 3 H); 3.6–3.75 ppm (t; 2 H); 3.8–3.95 ppm (m; 2 H); 4.8–4.9 ppm (t; 1 H); 7.35–7.8 ppm (m; 4 H).

IR (KBr pellet): $\tilde{\nu} = 3516$ cm^{-1} (—OH); 2216 cm^{-1} (—C \equiv N).

UV/Vis (THF): $\lambda_{\text{max}} = 326$ nm; $\epsilon = 23200$ $\text{l mol}^{-1} \text{cm}^{-1}$.

| | | | | |
|---|-------|---------|--------|---------|
| $\text{C}_{10}\text{H}_{12}\text{N}_4\text{O}$ (204.23) | calc. | C 58.81 | H 5.92 | N 27.43 |
| | found | C 58.89 | H 6.01 | N 26.98 |

Synthesis of triazene-containing polymers

PMMA copolymer I containing triazene functional groups in the side-chain

The copolymer is prepared by polymer analogous reaction. The synthesis is carried out in a 100 ml flask under nitrogen atmosphere. 10.05 g of a copolymer of methacrylic acid chloride and methyl methacrylate (molar ratio 9:1) are dissolved in 70 ml of dioxane. The solution is treated with 2.04 g (0.01 mol) of 1-(4-cyanophenyl)-3-(2-hydroxyethyl)-3-methyltriazene and 2.02 g (0.03 mol) of pyridine. The homogeneous reaction mixture is stirred in the dark for 72 h, filtered, and the polymer is precipitated in methanol. The light yellow polymer is purified twice, by dissolution in THF and precipitation by methanol addition, and dried in vacuo over diphosphorus pentoxide.

$^1\text{H NMR}$ (CDCl_3): $\delta = 0.75 - 1.15$ ppm (m; $-\text{CH}_3$); $1.75 - 2.10$ ppm (m; $-\text{CH}_2-$); $3.40 - 3.60$ (s; $-\text{OCH}_3$); $7.25 - 7.60$ ppm (m; aryl).

IR (KBr pellet): $\tilde{\nu} = 2216$ cm^{-1} ($-\text{C}\equiv\text{N}$); 1732 cm^{-1} ($\text{C}=\text{O}$).

UV/Vis (THF): $\lambda_{\text{max}} = 321$ nm; $\epsilon = 66$ l mol $^{-1}$ cm $^{-1}$.

The extent of derivatization of the MMA/methacrylic acid chloride (10 mol-%) copolymer by polymer analogous reaction was determined IR-spectroscopically, by monitoring the decrease of the $\text{C}=\text{O}$ stretching band of the acid chloride. 40% of the acid chloride was observed to react according to this method, which would correspond to a triazene content of 4%. However, if the low value of the molar absorption coefficient ($\epsilon = 66$) measured for the polymer redissolved in THF is ratioed to the absorption coefficient of the triazene monomer, a triazene content of only 0.3% is obtained for the copolymer. Apparently, a large fraction of the triazene groups has been decomposed during the polymers analogous reaction or during the subsequent processing steps.

Polymer TP 1 containing the triazene functional group in the main-chain

0.01 mol of 1-(3-carboxyphenyl)-3-(2-hydroxyethyl)-3-methyltriazene, 0.015 mol of $\text{N,N}'$ -dicyclohexylcarbodiimide, and 2 mmol of dimethylaminopyridine are dissolved in 30 ml of dry THF. The reaction mixture is stirred at 50°C for 48 h. Subsequently, 1 ml of distilled water is added to complete the hydrolysis of the $\text{N,N}'$ -dicyclohexylcarbodiimide, and the mixture is stirred for additional 12 h.

A precipitate of $\text{N,N}'$ -dicyclohexyl-urea is removed by filtration. The solution containing the product is dried over sodium sulfate, and the polymer is precipitated with n -hexane. The resulting product is dried in vacuo over diphosphorus pentoxide.

T. Lippert, A. Wokaun, J. Stebani, O. Nuyken, J. Ihlemann

^1H NMR (DMSO- d_6): $\delta = 3.10\text{--}3.35$ ppm (m; 3H); $4.00\text{--}4.25$ ppm (m; 2H); $4.40\text{--}4.60$ ppm (m; 2H); $7.15\text{--}7.85$ ppm (m; 4H).

IR (KBr pellet): $\tilde{\nu} = 1720$ cm^{-1} (C=O).

UV/Vis (THF): $\lambda_{\text{max}} = 288$ nm; $\epsilon = 14250$ $\text{l mol}^{-1} \text{cm}^{-1}$.

Polymer TP 2 containing the triazene functional group in the main-chain

This polymer is synthesized by interfacial polycondensation. 2.00 g (0.01 mol) of bis(4-aminophenyl)ether is dissolved in 20 ml of 10% hydrochloric acid. The mixture is cooled to -5 °C in a dry ice/acetone bath, a cooled solution of 1.38 g (0.02 mol) of sodium nitrite in 5 ml of distilled water is added, and the reaction mixture is stirred for five minutes. The resulting bis-diazonium-salt solution is treated with a cooled solution of 10.0 g of sodium carbonate in 50 ml of distilled water. Under vigorous stirring, a solution of 1.44 g (0.01 mol) of 1,6-bis(methylamino)-hexane in 50 ml n-hexane is added to the reaction mixture. The polycondensation is completed after 15 min. The light-beige polymer is filtered, washed with water and hexane, and dried in vacuo over diphosphorus pentoxide.

^1H NMR (DMSO- d_6): $\delta = 1.2\text{--}1.4$ ppm (m; 4H); $1.5\text{--}1.8$ ppm (m; 4H); $3.0\text{--}3.2$ ppm (s; 6H); $3.6\text{--}3.8$ ppm (t; 4H); $6.8\text{--}7.4$ ppm (m; 8H).

IR (KBr pellet): $\tilde{\nu} = 2926$ cm^{-1} (CH_2); 1492, 1354, and 1234 cm^{-1} .

UV/Vis (THF): $\lambda_{\text{max}} = 330$ nm; $\epsilon = 33000$ $\text{l mol}^{-1} \text{cm}^{-1}$.

Formation of the polymer films

0.5 g of the polymer is dissolved in 10 ml of dry THF. The solution is poured into a flat glass dish with a diameter of 4.5 cm and a bottom of good planarity. After 24 h, the polymer film is cut out of the dish and dried for additional 24 h in vacuo. The films produced in this manner have a thickness of ≈ 200 μm .

Results

Upon irradiation at 308 nm, a distinctly different behaviour has been observed with the three investigated polymers.

The copolymer I containing 0.3 mol-% of triazene-containing side chains is similar in its ablation characteristics to PMMA polymers that have been physically doped with low concentrations of monomeric triazene compounds^{5,6}. Scanning electron micrographs (Fig. 1) of the irradiated spots

reveal the presence of deep craters, with an ablated depth of up to 32 μm per pulse at 10.7 J cm^{-2} fluence. These craters exhibit a rough profile, with molten material and solidified bubbles at the bottom and the edges, and large quantities of ejected material in a circle around the crater. At lower fluences ($\leq 6 \text{ J cm}^{-2}$), no craters are created; instead, convex mounds are appearing on the surface (Fig. 2).

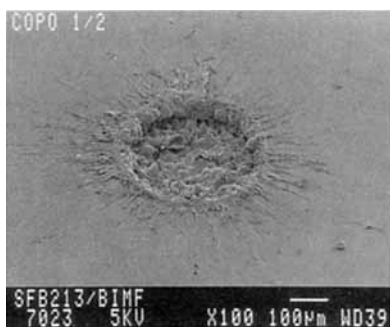


Fig. 1.

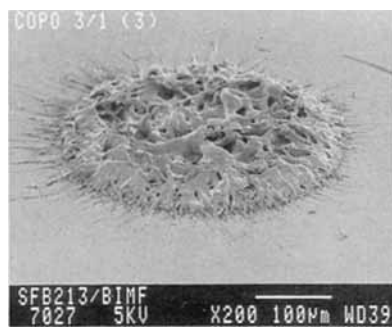


Fig. 2.

Fig. 1. Excimer laser-induced ablation of copolymer I at 308 nm. The ablated crater, as shown in the scanning electron micrograph, was produced by two laser pulses of 10.7 J cm^{-2} fluence.

Fig. 2. Excimer laser-induced ablation of copolymer I at 308 nm. The convex mound was produced by one laser pulse of 6.15 J cm^{-2} fluence.

Irradiation of the triazene polymer TP 1 results in wide and ill-defined craters (Fig. 3). Note that the affected area in Fig. 3 has an outer diameter of $\approx 900 \mu\text{m}$, while the diameter of the laser beam corresponded only to 375 μm .

The triazene polymer TP 2 exhibits a different ablation characteristics. Electron micrographs (Fig. 4) of the ablated craters exhibit well-defined

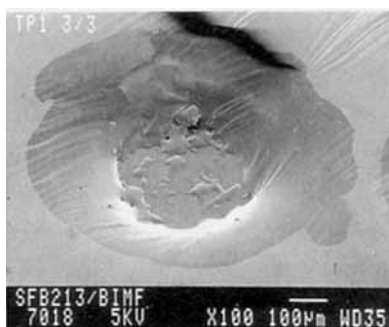


Fig. 3. Excimer laser-induced ablation of triazene polymer TP 1 at 308 nm. The ablated crater was produced by two laser pulses of 7 J cm^{-2} fluence.

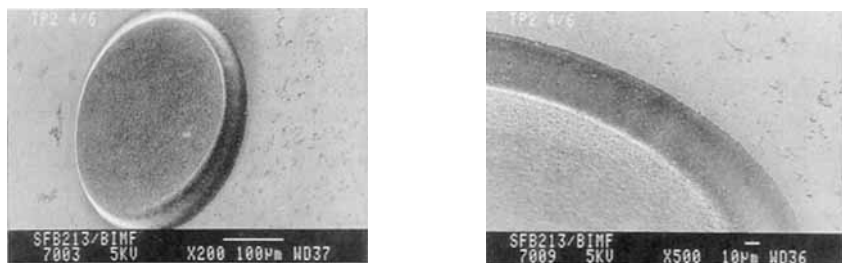


Fig. 4. Excimer laser induced ablation of triazene polymer TP 2 at 308 nm. The ablated crater, of 56 μm depth, was produced by 40 laser pulses of 1.7 J cm^{-2} fluence.

profiles with perfectly circular contours, steep edges, and flat bottom surfaces of the crater. The ablated depth per pulse shows a regular and reproducible dependence on laser fluence (Fig. 5). At a given pulse energy, the total ablated depth increases linearly with the number of pulses delivered (Fig. 6). Thus, in the range of fluences used there are no indications for an incubation phenomenon as had been observed with other polymers (i. e., a minimum number of incubation pulses required prior to the onset of ablation⁷): For TP 2, the linear regression lines representing ablated depth as a function of pulse number (Fig. 6) are all passing through the origin, and hence no incubation pulses are required.

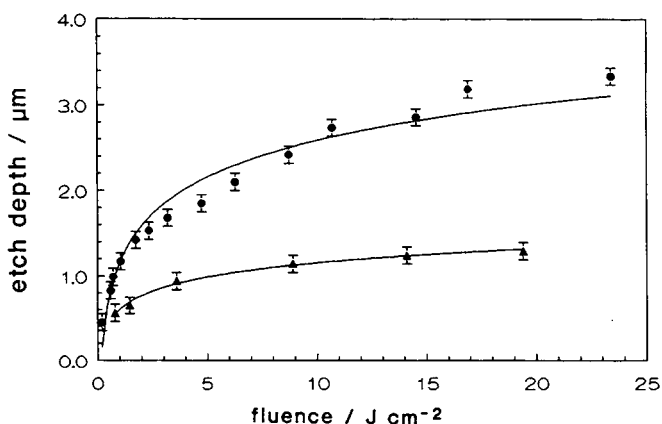


Fig. 5. Ablated depth per pulse as a function of laser fluence for polymer TP 2. The etched depth per pulse is plotted as a function of laser fluence at 308 nm (\bullet) and at 248 nm (\blacktriangle), respectively.

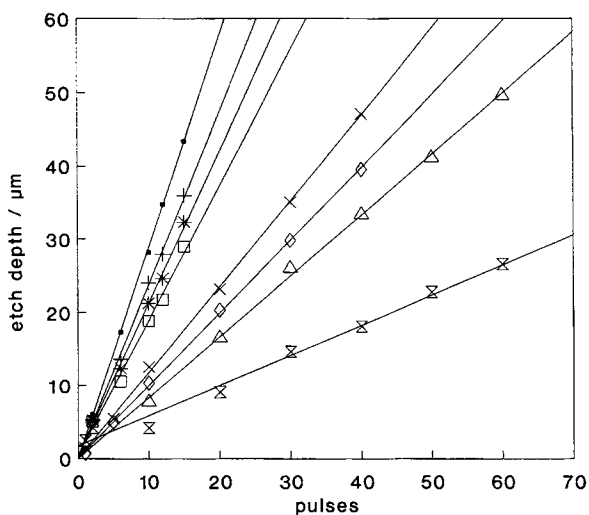


Fig. 6. The etched depth of polymer TP 2 plotted as a function of the number of excimer laser pulses at 308 nm, for various fluences ($J\text{ cm}^{-2}$): (●) 14.545, (+) 8.73, (*) 6.27, (□) 4.75, (×) 1.05, (◇) 0.70, (△) 0.59, (⊗) 0.2.

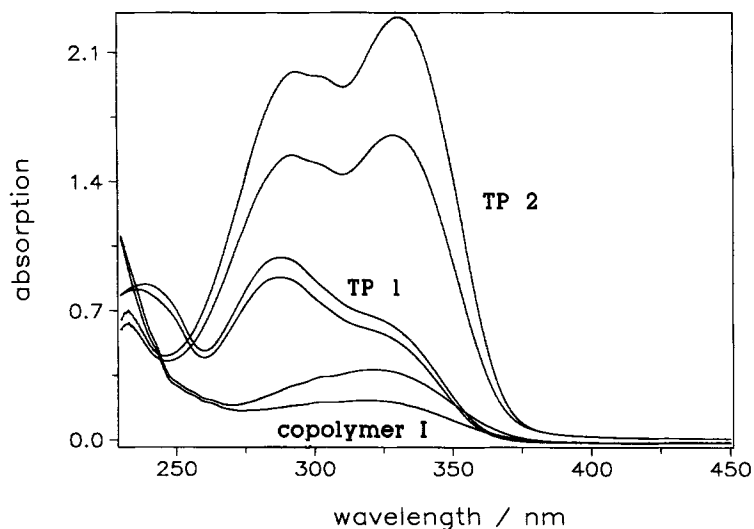


Fig. 7. Photolysis of triazene polymer TP 2 (7×10^{-5} M, top two curves), polymer TP 1 (7×10^{-5} M, middle) and of the copolymer I (6×10^{-3} M, bottom) in THF solution. For each polymer, absorption curves are plotted before and after irradiation with 50 excimer laser pulses, of 80 mJ energy at 308 nm.

The different ablation behaviour of the three polymers can not be ascribed to a difference in photolysis quantum yields in solution. Results of excimer laser photodecomposition experiments at 308 nm in THF solution are shown in Fig. 7. The copolymer I has a photolysis quantum yield of $\approx 0.19 \pm 0.12\%$ (as referred to the molar absorption coefficient of the monomer), the triazene polymer TP 1 a yield of $\approx 0.28\%$, and the polymer TP 2 a yield of $\approx 0.215\%$.

The ablated depth per pulse depends on an inverse power of the molar absorption coefficient. For the copolymer ($\epsilon = 61$ at 308 nm, which correspond to a triazene content of 0.3%) very high etch rates are achieved. For the highest laser fluences used (10.7 J cm^{-2}), ablated depths of up to $32 \text{ }\mu\text{m/pulse}$ have been achieved, although some bubbles appear at the walls and on the bottom of the crater under these conditions. For polymer TP 1 ($\epsilon = 11\,000$ at 308 nm) an etch depth of $\geq 4 \text{ }\mu\text{m}$ per pulse of 7 J cm^{-2} fluence was estimated from the profiles, which are not well defined. Polymer TP 2, which exhibits the highest molar absorption coefficient ($\epsilon = 28\,000$ at 308 nm) exhibits a limiting etch depth of $\approx 3.2 \text{ }\mu\text{m/pulse}$.

Wavelength dependence

The ablation characteristics of the main chain triazene polymer TP 2 at 248 and 308 nm are compared in Fig. 5, in which the etch depth per pulse is plotted as a function of laser fluence for both 248 and 308 nm excitation. The behaviour is significantly different from the one of undoped polymers such as PMMA or polystyrene, which are efficiently ablated at 248 nm, and do not exhibit ablation at 308 nm. For TP 2, the limiting etch depth per pulse is $\approx 3 \text{ }\mu\text{m}$ at 308 nm, as compared to $\approx 1 \text{ }\mu\text{m}$ at 248 nm. This observation indicates that the triazene photolysis, rather than depolymerization or other mechanisms which have been proposed as ablation mechanisms⁸, is essential for the ablation of TP 2.

Discussion

The observed difference between 248 and 308 nm ablation is not simply related to the photophysical parameters of the polymer in tetrahydrofuran solution. First, the photolysis quantum yield in solution at 248 nm (1.5%) is higher than the one at 308 nm (0.22%). Second, according to current theories⁹ of laser ablation, the ablated depth per pulse, d (F), at a given fluence, F , is inversely proportional to the linear absorption coefficient, α ,

$$d(F) = \frac{1}{\alpha_{\text{eff}}} \ln \frac{F}{F_0}, \quad (1)$$

where F_0 is the threshold fluence for ablation. However, although the absorption coefficient in solution at 248 nm is smaller than the one at 308 nm, the ablated depth per pulse at 248 nm is smaller as well, i.e. contrary to expectation.

To obtain some insight into the origin of this behaviour, the dependence of ablated depth on fluence for both wavelengths has been represented according to Eq. (1) in logarithmic plots, shown in Fig. 8. From a least squares fit, the following results have been obtained:

$$308 \text{ nm: } \alpha_{\text{eff}} = (1.83 \pm 0.03) \times 10^4 \text{ cm}^{-1}; F_0 = 114 \pm 20 \text{ mJ cm}^{-2};$$

$$248 \text{ nm: } \alpha_{\text{eff}} = (4.13 \pm 0.10) \times 10^4 \text{ cm}^{-1}; F_0 = 91 \pm 30 \text{ mJ cm}^{-2}.$$

While the threshold fluences, F_0 , are similar for both wavelengths, the effective absorption coefficient α_{eff} at 248 nm is higher by a factor of 2.3, in agreement with the observed high fluence limit on the etch depth per pulse, which is smaller roughly by the same factor.

Two tentative explanations might be proposed to account for the observed behaviour. First, saturation effects due to the intense excimer laser pulse might lead to saturation effects in the strong absorption band at 308 nm. A laser-induced bleaching of the absorption would be equivalent to a reduction of the effective absorption coefficient relevant for the absorption. Alternatively, it is conceivable that upon irradiation with higher photon energies at 248 nm, strongly absorbing photoproducts are generated during the initial period of the pulse, which would increase the effective absorption coefficient, and prevent the later parts of the pulse from penetrating into the polymer sample. Further work will be required to confirm the validity of either of the two models.

The main chain triazene polymer TP 2 ($M_w \approx 100000$) exhibits a behaviour as expected for a strongly absorbing polymer. The comparatively high maximum etch depth per pulse ($\approx 3 \mu\text{m}$) may be due to the fact that the polymer contains the photolabile triazene group, from which nitrogen is released during UV irradiation. The nitrogen acts as a driving gas to promote the ejection of material. The unusual wavelength dependence (Fig. 8) appears to indicate that the selective bond breaking releasing N_2 is more effective from the state excited at 308 nm. Such a wavelength dependent photolysis behaviour has recently been deduced from the wavelength dependent photolysis

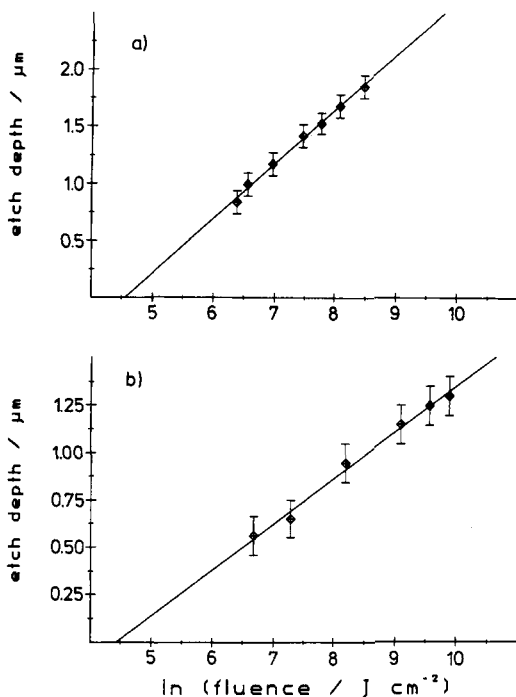


Fig. 8. Dependence of the ablated depth per pulse on the logarithm of laser fluence, for irradiation wavelengths of 308 nm (a) and 248 nm (b), respectively.

behaviour of monomeric methoxy-phenyl-azosulfonates in solution¹⁰. The generation of nitrogen driving the ablation would also account for the observation that no incubation pulses are necessary in the fluence range used.

With polymer TP 1, the profiles are not sufficiently well defined for a quantitative depth analysis from profilometer traces. From optical and electron microscope pictures, the holes appear to be deeper than the ones observed with TP 2. Two reasons can be indicated for these differences. First, the absorption coefficient of TP 1 is smaller, and hence the penetration depth of the UV laser beam into the polymer is higher. Second, the glass temperature of TP 1 ($T_g = 298 \pm 5$ K) and the molecular weight ($M_w \approx 2000$) are lower than the corresponding values of TP 2 ($T_g = 336 \pm 5$ K, $M_w \approx 100000$). As a consequence, polymer TP 1 has a much higher tendency to flow as a consequence of the temperature rise induced by the irradiation. This accounts

for the observation (Fig. 3) that no sharp crater edges can be achieved with TP 1.

The copolymer I exhibits a behaviour similar to the one of PMMA doped with monomeric triazene compounds^{5,6}. A quantitative interpretation is impeded from an unresolved discrepancy in the content of triazene (4% from elemental analysis; 0.3% from UV analysis). The recorded etch depths, the observation of convex mounds at lower fluences, and the rough profiles of the craters would be consistent with a triazene content of 0.3%. For dopant concentration exceeding 2%, more shallow craters and better defined profiles are usually observed.

A significant difference between doped polymers^{4,5,6} and the copolymer I, in which the triazene group is bound to the polymer backbone through an ester functionality, is the appearance of abundant bubbles in the crater. A possible explanation may invoke a radical decomposition mechanism of triazene photolysis¹¹. The $-\text{CH}_2-\text{CH}_2-\text{N}^{\bullet}-\text{CH}_3$ radical, which resides on the polymer chain after photochemical bond cleavage at the triazene group and release of N_2 , may react with other radicals, atmospheric oxygen, or moisture, to form the bubbles.

Conclusions

Three different triazene polymers have been compared in this study with respect to their laser-induced ablation behaviour at 308 nm. The PMMA copolymer I containing 0.3% of triazene side chains does not yield satisfactory ablation profiles.

Among the main-chain triazene polymers, TP 1 has the lowest molecular weight (≈ 2000). The ablation craters achieved with this polymer do not yield an acceptable quality of the ablation profiles (cf. Fig. 3).

The polymer TP 2 exhibits the most favorable properties with respect to ablation. The material is synthesized by a relatively simple procedure. The polymer obtained is characterized by a comparatively high molecular weight ($M_w \approx 100000$), and is well soluble in organic solvents such as THF and cyclohexanone. It exhibits a high temperature stability (up to 282 °C). Upon 308 nm irradiation of TP 2, well-defined ablation craters with sharp edges, clean contours and flat bottoms are obtained. The material appears therefore well suited for applications in photolithographic processes.

The fluence dependence of the ablated depth per pulse has been investigated for both 308 and 248 nm irradiation. Interestingly, the high fluence limit at 308 nm ($\approx 3 \mu\text{m}/\text{pulse}$) exceeds the one at 248 nm ($\approx 1 \mu\text{m}/\text{pulse}$). This behaviour

is different from the one observed with most undoped polymers, and is attributed to the specific ablation mechanism which is active for the triazene polymers. Nitrogen which is released in the course of the triazene photochemical decomposition is thought to act as a driving gas for the ejection of material from the irradiated area. Further investigations of these aspects are in progress in our laboratory.

We are indebted to K. Luther for stimulating discussions, and to C. Drummer for recording the scanning electron micrographs. Financial support of this work by grants of the Deutsche Forschungsgemeinschaft (SFB 213) and of the BMFT (grant 13N5621-5) is gratefully acknowledged.

- ¹ Y. Kawamura, K. Toyoda, S. Namba, *Appl. Phys. Lett.* **40** (1982) 374
- ² R. Srinivasan, V. Mayne-Banton, *Appl. Phys. Lett.* **41** (1982) 576
- ³ G. E. Wolbold, E. Roth, W. Stoeffler, J. R. Lankard, *Proc. Laserion Conference, Munich, 12.-14. 6. 1991*, p. 75; J. R. Lankard Sr., G. Wolbold, *Appl. Phys. A* **54** (1992) 355
- ⁴ R. Srinivasan, B. Braren, R. W. Dreyfus, L. Hadel, D. E. Seeger, *J. Opt. Soc. Am.* **B 3** (1986) 785
- ⁵ M. Bolle, K. Luther, J. Troe, J. Ihlemann, H. Gerhardt, *Appl. Surf. Sci.* **46** (1990) 279
- ⁶ T. Lippert, J. Dauth, J. Stebani, O. Nuyken, A. Wokaun, J. Ihlemann, to be published 1993
- ⁷ S. Küper, M. Stuke, *Appl. Phys. A* **49** (1989) 211
- ⁸ D. Dijkamp, A. S. Gozdz, T. Venkatesan, X. D. Wu, *Phys. Rev. Lett.* **58** (1987) 2142
- ⁹ V. Srinivasan, M. A. Smrtic, S. V. Babu, *J. Appl. Phys.* **59** (1986) 3861
- ¹⁰ D. Franzke, B. Voit, O. Nuyken, A. Wokaun, *Mol. Phys.* **77** (1992) 397
- ¹¹ J. Baro, D. Dudek, K. Luther, J. Troe, *Ber. Bunsen-Ges. Phys. Chem.* **87** (1983) 1155, 1161